month and numerous admissions to psychiatric units. At the age of 31, she was admitted to our psychiatric hospital. Since she was admitted to our psychiatric hospital, we observed her mood episodes for more than one year. During this period, in all of her menstrual cycles (MCs), the patient demonstrated manic episodes regularly beginning at around day 7 in the follicular phase. Her manic episodes continued for about two weeks, around ovulation, with euthymic state intervals. She had a natural 28-day menstrual cycle and did not take oral contraceptives at all during her recurrent manic/mood episodes. We diagnosed her as rapid-cycling bipolar disorder based on the structured clinical interview for DSM-IV axis I disorder (SCID) (First et al., 1997). We tried several mood-stabilizing medications, electroconvulsive therapy (ECT) treatments, but her manic episodes continued to recur.

To examine the mechanisms underlying the illness phases related to the menstrual cycle, the serum levels of estradiol and progesterone were analyzed twice: first at the euthymic state before the manic state (day 23 of MC), and second at the manic state (day 12 of MC). To replicate the relation of the gonadal hormones and the manic state, we performed a second analysis of gonadal hormones during another menstrual cycle [first at euthymic state (day 2 of MC), and second at manic state (day 12 of MC)].

For the purpose of investigating brain microstructural changes in manic episode compared to before and after manic episode, DTI was performed three times: first at the euthymic state before the manic state (day 23 of MC), second at the manic state (day 12 of MC), and third at the euthymic state following the previous manic state (day 2 of MC). We could not do further imaging analysis for replicating the results because of refusal by the patient. During the analyses of serum gonadal hormones and MRI scans, the patient was in a drug-free condition, taking no mood stabilizers or antipsychotic drugs.

Thirty-four healthy control subjects (11 female/23 male, age: 28.3 ± 6.4 years) were recruited from the local area by poster advertisement. Exclusion criteria for healthy subjects were a history or present diagnosis of any DSM-IV axis I diagnosis or any neurological illness. The patient and controls were subjected to a series of standardized, quantitative measurements of manic and depressive symptoms [Young Mania Rating Scale (YMRS) (Young et al., 1978), Montgomery Asberg Depression Rating Scale (MADRAS) score (Montgomery and Asberg, 1979), and Hamilton Rating Scale for Depression (HAMD-17) (Hamilton, 1960)] on the day of the MRI scan.

After complete description of the study, written informed consent was obtained from the patient and the healthy controls. The study was approved by the medical ethics committee of the National Cerebral and Cardiovascular Center in Japan.

2.2. Hormone assay

Blood was withdrawn via the median antebrachial vein. Sera were separated by centrifugation at 3200 rpm for 7 min and sent to Ikagaku CO., LTD (Kyoto, Japan), where the serum concentrations of estradiol and progesterone were measured by direct chemiluminescence, using Siemens ADVIA® Centaur™ Immunoassay System. For normal ranges of estradiol and progesterone for the menstrual phase, we used the laboratory data provided by Ikagaku CO., LTD determined from multiple subjects.

2.3. Data acquisition of MRI

All MRI examinations were performed by 3-Tesla whole-body scanner (Signa Excite HD V12M4; GE Healthcare, Milwaukee, WI, USA) with an 8-channel phased-array brain coil. Diffusion-weighted MR images were obtained with a locally modified single-shot echo-planar imaging (EPI) sequence by parallel acquisition at a reduction (ASSET) factor of 2, in the axial plane. Imaging parameters were as follows: TR = 17 s; TE = 72 ms; b = 0, 1000 s/mm^2; acquisition matrix, 128 × 128; field of view (FOV), 256 mm; section thickness, 2.0 mm; no intersection gap; 74 sections. The reconstruction matrix was the same as the acquisition matrix, and 2 mm × 2 mm × 2 mm isotropic voxel data were obtained. Motion probing gradient (MPG) was applied in 55 directions, the number of images was 4144, and the acquisition time was 15 min and 52 s.

To reduce blurring and signal loss arising from field inhomogeneity, an automated high-order shimming method based on spiral acquisitions was used before acquiring the DTI scans. To correct for motion and distortion from eddy current and B0 inhomogeneity, FMRIB software (FMRIB Center, Department of Clinical Neurology, University of Oxford, Oxford, England; http://www.fmrib.ox.ac.uk/fsl/) was utilized. B0 field mapping data were also acquired with the echo time shift (of 2.237 ms) method based on two gradient echo sequences.

High-resolution three-dimensional T1-weighted images were acquired using a spoiled gradient-recalled sequence (TR = 12.8 ms, TE = 2.6 ms, flip angle = 8°, FOV, 256 mm; 188 sections in the sagittal plane; acquisition matrix, 256 × 256; acquired resolution, 1 × 1 × 1 mm^3). T2-weighted images were obtained using a fast-spin echo (TR = 4800 ms; TE = 101 ms; echo train length (ETL) = 8; FOV = 256 mm; 74 slices in the transverse plane; acquisition matrix, 160 × 160, acquired resolution, 1 × 1 × 2 mm^3).

2.4. Imaging processing

FA images and three eigenvalues ($\lambda1$, $\lambda2$, and $\lambda3$) were generated from each individual using FMRIB software. First, brain tissue was extracted using the Brain Extraction Tool in FSL software. Diffusion-weighted images for each of the 55 directions were eddy-corrected, subsequent to which FA values were calculated at each voxel using the FSL FMRIB Diffusion Toolbox.

Image preprocessing and statistical analysis were carried out using SPM8 (Wellcome Department of Imaging Neuroscience, London, England). Each subject's echo planar image was spatially normalized to the Montreal Neurological Institute echo planar image template using parameters determined from the normalization of the image with a b value of 0 s/mm^2 and the echo planar image template in SPM8.

Normalized gray and white matter images were generated from each individual T1-weighted image using the VBM8 toolbox with SPM8 software (Ashburner and Friston, 2000).

Normalized images were spatially smoothed using an isotropic Gaussian filter (6-mm full-width at half-maximum).

2.5. Voxel-based analysis

Exploratory voxel-based analysis was performed using SPM8 software. FA and gray/white matter images were compared between the patient and healthy subjects with Jack-knife analysis. Statistical inferences were made with a voxel-level threshold of $p < 0.05$, after family-wise error correction for multiple comparisons, with a minimum cluster size of 50 voxels.

Spherical VOIs (3-mm radius) were determined from regions where the patient showed significantly higher or lower FA values than controls. The center of the spherical VOIs was determined from the MNI coordinate with peak t-value. The regional FA value was calculated by averaging values for all voxels within the spherical VOIs placed on the regions of FA images of controls and patient at euthymic and manic states. The same VOIs were applied to $\lambda1$, $\lambda2$ and $\lambda3$ images. $\lambda1$–$\lambda3$ Values were extracted, and mean diffusivity (MD) [($\lambda1+\lambda2+\lambda3$)/3], axial ($\lambda1$) and radial diffusivity ([$\lambda2+\lambda3$]/2) were compared (Alexander et al., 2007).

To examine the effect of age on white matter integrity in our study, we examined the relationship between the regional FA values in the VOIs and age by Pearson's correlation analysis. To assess the effect of gender on white matter integrity in our study, we compared the regional FA values between male and female controls by t-test.

3. Results

3.1. Demographic and clinical data

Table 1 summarizes the demographic and clinical characteristics of the patient and controls. Manic and depressive symptoms were assessed on the day of the MRI session at euthymic and manic states. The patient showed manic symptoms at only manic states, and no manic or depressive symptoms at euthymic states. None of the control subjects showed manic or depressive symptoms at the examination.

3.2. Estradiol and progesterone levels in the patient's blood

As shown in Table 2, because of the normal menstrual cycle phase, estradiol levels increased in the late follicular phase at manic state when compared to the luteal or early follicular phase

Table 1
Demographic characteristics of the analysis of the patient and controls.

Characteristic	Patient	Controls (n = 34)
Age, y	33	28.3 ± 6.4
Female, No (%)	–	11 (32%)
Young Mania Rating Scale	0 At euthymic state 42 at manic state	0 For all controls
MADRAS score	0 At both states	1.0 ± 1.7
HAM-D score	0 At both states	1.1 ± 1.6

MADRAS, Montgomery Asberg Depression Rating Scale; HAM-D, Hamilton Depression Rating Scale.

Table 2
Serum levels of estradiol and progesterone at euthymic and manic states.

Hormone	Euthymic state	Menstrual phase (day of cycle)	Manic state	Menstrual phase (day of cycle)
Estradiol (pg/mL) (normal range for menstrual phase)				
First test	87.4 (55.8–214.2)	Luteal (23)	512 (63.9–356.7)	Late follicular (12)
Second test	41 (19.5–144.2)	Early follicular (2)	206 (63.9–356.7)	Late follicular (12)
Progesterone (ng/mL) (normal range for menstrual phase)				
First test	15.2 (1.4–20.6)	Luteal (23)	< 0.2 (0.3–10.4)	Late follicular (12)
Second test	0.8 (< 1.2)	Early follicular (2)	0.2 (0.3–10.4)	Late follicular (12)

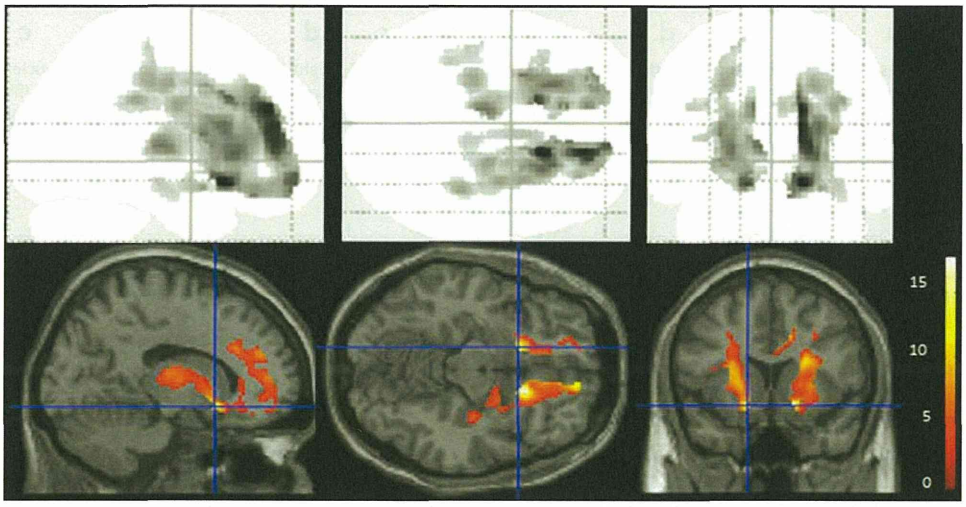

Fig. 1. Regions with significant differences in FA values between controls and the patient at manic state. Sagittal, coronal, and transverse brain views show voxels with significantly higher FA values in the patient at manic state when compared to controls. Detected areas shown in this figure exceed an uncorrected p value of 0.001 with 100 or more contiguous voxels. These statistical parametric mapping projections were then superimposed on representative sagittal ($x=-14$), coronal ($y=-12$), and transverse ($z=14$) magnetic resonance images.

Table 3
Regional change of FA values related to manic state of the patient.

Comparison	Region	MNI coordinates (x, y, z)	Voxels	t-Value	p-Value (FWE-corrected)
Patient < controls	None				
Patient > controls	Right nucleus accumbens	16, 18, −12	1458	17.84	< 0.001
	Left nucleus accumbens	−14, 14, −12	1053	14.25	< 0.001
	Left thalamus	−8, −16, 8	154	10.77	< 0.001

MNI: Montreal Neurological Institute; FWE-corrected: familywise error-corrected.

at euthymic state. The serum progesterone level was lower in the late follicular phase than those in the luteal and early follicular phase, although the difference in levels between the late and early follicular phase was small in the second test.

In the late follicular phase at manic state, one of the two tested estradiol levels was above the reference range and the two tested progesterone levels were below the reference range, although the deviations of the progesterone levels from the reference range were small. In the early follicular and luteal phase at euthymic state, the two tested estradiol and progesterone levels were within the reference range.

3.3. Comparisons of FA values between the patient and controls by voxel-based analysis

In the voxel-based analysis of FA values, the patient at manic state showed significantly higher FA values in the bilateral nucleus accumbens (NAc) and left thalamus. We found no significantly lower FA values in the patient. The areas of the higher FA values, shown in Fig.1, extended from NAc to the bilateral medial frontal region, anterior cingulate, thalamus, and right amygdala and hippocampus. We found no significant differences in FA values between the patient and healthy subjects at euthymic state. There were no significant differences in gray/white matter volumes between healthy subjects and the patient at manic and euthymic states.

3.4. Difference in patient FA values between manic and euthymic states

Spherical volumes of interest (VOIs) were placed on the bilateral NAc and left thalamus where the significant differences between the patient and controls were shown by voxel-based analysis (Table 3). The exact FA values of each area of the patient and controls at manic and euthymic states are shown in Fig. 2 and Table 4. The patient showed significantly increased FA values compared to controls (> mean + 2 S.D. of controls) only at manic state in these VOIs. We found no significant relationship between age and regional FA values in the control group by correlation

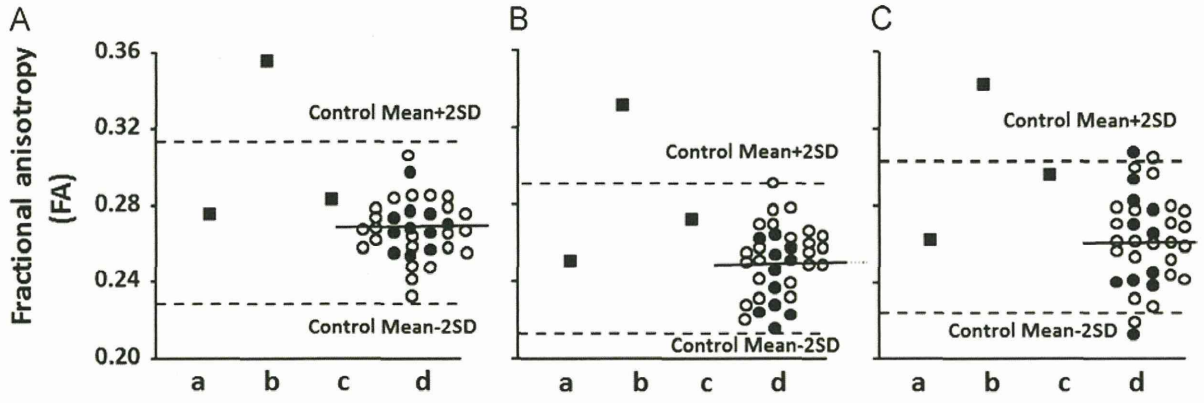

Fig. 2. Scatter plots of the FA values of the controls and patient with euthymic and manic states. (A) Right nucleus accumbens; (B) Left nucleus accumbens; and (C) Left thalamus: (a) Euthymic state (1st test); (b) Manic state (2nd test); (c) Euthymic state (3rd test) and (d) Controls ($n=34$). Filled squares: patient, filled circles: female controls, open circles: male controls. The FA values were derived from spherical VOIs (3-mm radius) placed on the regions with significant increases of FA values by voxel-based analysis (MNI coordinates are shown in Table 3). The exact FA values of each area of the patient and controls are also shown in Table 4. Significantly higher FA values of the patient than those of controls (> mean+2S.D. of controls) are shown only at manic state.

Table 4
FA values of the patient and controls.

	Mental state at MR imaging [menstrual phase (day of cycle)]	Right nucleus accumbens ($x, y, z=16, 18, -12$)	Left nucleus accumbens ($x, y, z=-14, 14, -12$)	Left thalamus ($x, y, z=-8, -16, 8$)
Patient	Euthymic state at 1st imaging [luteal (23)]	0.28	0.25	0.26
	Manic state at 2nd imaging [late follicular (12)]	0.36*	0.33*	0.34*
	Euthymic state at 3rd imaging [early follicular (2)]	0.29	0.27	0.30
Controls	(Mean ± S.D.)	0.27 ± 0.02	0.25 ± 0.02	0.26 ± 0.02

* Significantly different FA values of the patient from those of controls (< mean−2S.D. of controls, or > mean+2S.D. of controls).

Table 5
Values of mean diffusivity (MD), axial diffusivity (AD) and radial diffusivity (RD) ($\times 10^{-4}$) of the patient and controls.

	Mental state at MR imaging [Menstrual phase (day of cycle)]	Right nucleus accumbens ($x, y, z=16, 18, -12$)			Left nucleus accumbens ($x, y, z=-14, 14, -12$)			Left thalamus ($x, y, z=-8, -16, 8$)		
		MD	AD	RD	MD	AD	RD	MD	AD	RD
Patient	Euthymic state at 1st imaging [luteal (23)]	2.19	9.01	5.37	2.28	8.49	6.02	2.36	8.51	6.36
	Manic state at 2nd imaging [late follicular (12)]	2.39	10.5*	5.54	2.39	9.95*	5.80	2.62	10.6*	6.51
	Euthymic state at 3rd imaging [early follicular (2)]	2.37	9.66	5.83	2.31	9.02	5.91	2.27	8.86	5.79
Controls	(Mean ± S.D.)	2.27 ± 0.13	8.90 ± 0.51	5.78 ± 0.41	2.27 ± 0.11	8.78 ± 0.42	5.81 ± 0.37	2.49 ± 0.11	9.37 ± 0.43	6.53 ± 0.37

* Significantly different values of the patient from those of controls (< mean−2S.D. of controls, or > mean+2S.D. of controls).

analysis. Regional FA values in the control group showed no significant difference between males and females (male vs. female, 0.27 ± 0.02 vs. 0.27 ± 0.01 in the right NAc, 0.25 ± 0.02 vs. 0.24 ± 0.02 in the left NAc, 0.26 ± 0.02 vs. 0.26 ± 0.03 in the left thalamus). Table 5 shows the quantification of the differences in the values of MD and radial/axial diffusivity in these regions. The patient showed significantly increased axial diffusivity compared to controls (> mean+2 S.D. of controls) only at manic state.

4. Discussion

DTI results showed that the patient had increased FA values compared to controls during mania in the bilateral NAc and its connected areas. The increased FA level of the patient at manic state was associated with increased axial diffusivity (AD). Diffusion MRI has been used to visualize dynamic tissue changes associated with neuronal activation (Darquié et al., 2001; Le Bihan et al., 2006). The mechanisms underlying water molecule diffusion changes observed by MRI still have not been entirely clarified (Jones et al., 2013), but it has been suggested that such diffusion changes might result from the peculiar properties of water in biological tissues, and from their association with the biophysical events underlying neuronal activity (Le Bihan, 2007). Increased FA values at manic state may reflect the microstructural changes due to the neuronal activation associated with manic episodes as shown in our patient.

Bilateral NAc and its connected areas play an important role in reward-related neural networks mediating motivation and goal-directed behavior (Salamone et al., 2007). Manic state has been characterized as abnormal goal pursuit regulation with elevated levels of achievement motivation and drive (Abler et al., 2008), and our finding of the change in reward-related neural networks could explain the manic symptoms in our patient. NAc is also a major projection field of the mesolimbic dopamine (DA) system (Deutch and Cameron, 1992). It has been hypothesized that abnormalities in dopaminergic neurotransmission may be important to the etiology of BPD (Anand et al., 2011). This hypothesis is supported by pharmacological evidence: psycho-stimulants can

produce symptoms similar to manic state (Gerner et al., 1976; Swann et al., 2004), and commonly used treatments for BPD have actions on post-synaptic dopamine signaling (Berk et al., 2007; Cousins et al., 2009). The hyper-activation of the mesolimbic DA system may have contributed to the abnormality of the reward-related neural networks in our patient.

The patient demonstrated manic episodes regularly at around day 7 of her MC, and they continued for about 2 weeks, with euthymic state intervals. Estradiol levels increased in the late follicular phase at manic state when compared to those in the luteal or early follicular phase at euthymic state. The serum progesterone level was lower in the late follicular phase than those in the luteal and early follicular phase, but the difference in levels was small, almost negligible, in the second test. On the other hand, in the late follicular phase at manic state, one of the two tested estradiol levels was within normal range. The two tested progesterone levels were below the reference range, but their deviations from the normal range were extremely small. According to these results, it is reasonable to assume that the elevation in the estradiol level due to the normal menstrual cycle has a consistent role in triggering the onset of manic symptoms, but abnormal levels of estrogen/progesterone were not necessary for the onset of manic symptoms.

In healthy females, functional MRI studies showed greater reactivity to reward during the follicular phase compared to the luteal phase of the menstrual cycle. A positive correlation between estradiol and reward-related activation of the bilateral amygdalo-hippocampal complex was also reported (Dreher et al., 2007). The result of our study was thought to be at least partly in agreement with their report.

A previous study has shown that the basal concentration of dopamine in rats is dependent on the circulating levels of estrogen (Becker, 1999). Czoty et al. examined the menstrual cycle-related changes of DA D2 receptor in female cynomolgus monkeys by using micro-PET with [^{18}F] fluoroclebopride (Czoty et al., 2009), and they found lower D2 distribution volume ratios in the follicular phase, which may be related to increases in DA release produced by high levels of estrogen (Becker et al., 2001; Dazzi et al., 2007). Our finding of a rise in the serum estradiol level due to a normal menstrual cycle and assumed hyper-activity of the mesolimbic DA system in the late follicular phase at manic state is in line with these previous studies. When considering that healthy women do not show manic symptoms due to a normal menstrual cycle, it is reasonable to suppose that the mesolimbic DA system of this patient specifically has abnormal hypersensitivity to the increase in the estradiol level from a normal menstrual cycle.

There are several points in this study that should be taken into consideration. First, our study is a single-case study and the results cannot be interpreted generally. Future larger-group designs are needed. Second, age should be regarded as the cause of heterogeneity of controls (Lebel et al., 2008; Kumar et al., 2013). However, we regarded their effect on our DTI results as relatively little, as we found no significant relationship between age and regional FA values in the control group. Third, our control group included twice as many males as females. The gender-related changes of white matter integrity were shown in healthy subjects in a recent study (Kumar et al., 2013). Although we confirmed that there was no statistical difference in FA in the VOIs between males and females of our controls, the large proportion of males in a relatively small sample was still insufficient to definitively rule out any difference. Further, the women in the sample were not assessed with regard to the stage of their menstrual cycle at the time of scanning. With a hypothesis based upon differences in brain structure due to the menstrual cycle, such factors could significantly affect the interpretation of the results. Future analysis with a restricted female control group assessed in regard to the menstrual cycle will be necessary for forming definitive conclusions. Fourth, it was reported that treated women with BPD do not seem to have menstruation-related mood symptoms (Payne et al., 2007; Shivakumar et al., 2008; Sit et al., 2011). During our analysis, the patient remained free of mood stabilizers / antipsychotic drugs, so we cannot directly compare our results with the previous reports of treated women with BPD. Finally, we did not measure the DA level. To the best of our knowledge, there has been no report about variations of the DA level in different mood states of BPD. However, the results of the present study tend to encourage us toward further investigations concerning the relation between the DA level and manic episodes in the human menstrual cycle.

In conclusion, we speculate that the mesolimbic DA system of this patient specifically has abnormal hypersensitivity to the increase in the estradiol level. According to our results, it is reasonable to suppose that the rise of the serum estradiol level in accord with the normal menstrual cycle increased the activity of the dopaminergic system and abnormally activated the reward-related neural networks, which may have contributed to the recurrent manic episodes in the patient. We may have unearthed a clue toward understanding how fluctuations in gonadal hormone production may amplify or ameliorate the symptomatology of psychiatric disorders characterized by altered mood and emotional states related to the menstrual cycle.

Financial support

This research was supported by the Japan Society for the Promotion of Science, Grant-in-Aid for Scientific Research (C), 24591740.

Acknowledgment

We would like to thank members of the MRI facility staff of the Department of Investigative Radiology, National Cerebral and Cardiovascular Center in Japan, for carrying out the acquisition of MRI data and taking care of all subjects during the MRI procedures.

References

Abler, B., Greenhouse, I., Ongur, D., Walter, H., Heckers, S., 2008. Abnormal reward system activation in mania. Neuropsychopharmacology 33, 2217–2227.
Akdeniz, F., Karadağ, F., 2006. Does menstrual cycle affect mood disorders? Turkish Journal of Psychiatry 17, 296–304.
Alexander, A.L., Lee, J.E., Lazar, M., Field, A.S., 2007. Diffusion tensor imaging of the brain. Neurotherapeutics 4, 316–329.
Anand, A., Barkay, G., Dzemidzic, M., Albrecht, D., Karne, H., Zheng, Q.H., Hutchins, G.D., Normandin, M.D., Yoder, K.K., 2011. Striatal dopamine transporter availability in unmedicated bipolar disorder. Bipolar Disorders 13, 406–413.
Ashburner, J., Friston, K.J., 2000. Voxel-based morphometry-the methods. NeuroImage 11, 805–821.
Becker, J.B., 1999. Gender differences in dopaminergic function in striatum and nucleus accumbens. Pharmacology Biochemistry and Behavior 64, 803–812.
Becker, J.B., Molenda, H., Hummer, D.L., 2001. Gender differences in the behavioral responses to cocaine and amphetamine. Implications for mechanisms mediating gender differences in drug abuse. Annals of the New York Academy of Sciences 937, 172–187.
Becker, O.V., Rasgon, N.L., Marsh, W.K., Glenn, T., Ketter, T.A., 2004. Lamotrigine therapy in treatment-resistant menstrually-related rapid cycling bipolar disorder: a case report. Bipolar Disorders 6, 435–439.
Berk, M., Conus, P., Lucas, N., Hallam, K., Malhi, G.S., Dodd, S., Yatham, L.N., Yung, A., McGorry, P., 2007. Setting the stage: from prodrome to treatment resistance in bipolar disorder. Bipolar Disorders 9, 671–678.
Cousins, D.A., Butts, K., Young, A.H., 2009. The role of dopamine in bipolar disorder. Bipolar Disorders 11, 787–806.
Czoty, P.W., Riddick, N.V., Gage, H.D., Sandridge, M., Nader, S.H., Garg, S., Bounds, M., Garg, P.K., Nader, M.A., 2009. Effect of menstrual cycle phase on dopamine D2 receptor availability in female cynomolgus monkeys. Neuropsychopharmacology 34, 548–554.
D'Mello, D.A., Pinheiro, A.L., Lalinec-Michaud, M., 1993. Premenstrual mania: two case reports. Journal of Nervous and Mental Disease 181, 330–331.

Darquié, A., Poline, J.B., Poupon, C., Saint-Jalmes, H., Le Bihan, D., 2001. Transient decrease in water diffusion observed in human occipital cortex during visual stimulation. Proceedings of the National Academy of Sciences of the United States of America 98, 9391–9395.

Dazzi, L., Seu, E., Cherchi, G., Barbieri, P.P., Matzeu, A., Biggio, G., 2007. Estrous cycle-dependent changes in basal and ethanol-induced activity of cortical dopaminergic neurons in the rat. Neuropsychopharmacology 32, 892–901.

Deutch, A.Y., Cameron, D.S., 1992. Pharmacological characterization of dopamine systems in the nucleus accumbens core and shell. Neuroscience 46, 49–56.

Dreher, J.C., Schmidt, P.J., Kohn, P., Furman, D., Rubinow, D., Berman, K.F., 2007. Menstrual cycle phase modulates reward-related neural function in women. Proceedings of the National Academy of Sciences of the United States of America 104, 2462–2470.

First, M.B., Spitzer, R.L., Gibbon, M., Williams, J.B.W., 1997. Structured Clinical Interview for DSM-IV (SCID-I)—Research Version. Biometrics Research, New York.

Gerner, R.H., Post, R.M., Bunney, W.E.J., 1976. A dopaminergic mechanism in mania. American Journal of Psychiatry 133, 1177–1180.

Hamilton, M., 1960. A rating scale for depression. Journal of Neurology, Neurosurgery & Psychiatry 23, 56–62.

Jones, D.K., Knösche, T.R., Turner, R., 2013. White matter integrity, fiber count, and other fallacies: the do's and don'ts of diffusion MRI. Neuroimage 73, 239–254.

Kukopulos, A., Minnai, G., Muller-Oerlinghausen, B., 1985. The influence of mania and depression on the pharmacokinetics of lithium. Journal of Affective Disorders 8, 159–166.

Kumar, R., Chavez, A.S., Macey, P.M., Woo, M.A., Harper, R., 2013. Brain axial and radial diffusivity changes with age and gender in healthy adults. Brain Research 1512, 22–36.

Le Bihan, D., 2007. The 'wet mind': water and functional neuroimaging. Physics in Medicine and Biology 52, R57–R90.

Le Bihan, D., Urayama, S., Aso, T., Hanakawa, T., Fukuyama, H., 2006Direct and fast detection of neuronal activation in the human brain with diffusion MRIProceedings of the National Academy of Sciences of the United States of America1038263-8268.

Lebel, C., Walker, L., Leemans, A., Phillips, L., Beaulieu, C., 2008. Microstructural maturation of the human brain from childhood to adulthood. NeuroImage 40, 1044–1055.

Montgomery, S.A., Asberg, M., 1979. A new depression scale designed to be sensitive to change. British Journal of Psychiatry 134, 382–389.

Payne, J.L., Roy, P.S., Murphy-Eberenz, K., Weismann, M.M., Swartz, K.L., McInnis, M. G., Nwulia, E., Mondimore, F.M., MacKinnon, D.F., Miller, E.B., Nurnberger, J.I., Levinson, D.F., DePaulo, J.R.J., Potash, J.B., 2007. Reproductive cycle-associated mood symptoms in women with major depression and bipolar disorder. Journal of Affective Disorders 99, 221–229.

Salamone, J.D., Correa, M., Farrar, A., Mingote, S.M., 2007. Effort-related functions of nucleus accumbens dopamine and associated forebrain circuits. Psychopharmacology (Berlin) 191, 461–482.

Shivakumar, G., Bernstein, I.H., Suppes, T.S.F.B.N., Keck, P.E., McElroy, S.L., Altshuler, L.L., Frye, M.A., Nolen, W.A., Kupka, R.W., Grunze, H., Leverich, G.S., Mintz, J., Post, R.M., 2008. Are bipolar mood symptoms affected by the phase of the menstrual cycle? Journal of Women's Health (Larchmt) 17, 473–478.

Sit, D., Seltman, H., Wisner, K.L., 2011. Menstrual effects on mood symptoms in treated women with bipolar disorder. Bipolar Disorders 13, 310–317.

Swann, A.C., Dougherty, D.M., Pazzaglia, P.J., Pham, M., Moeller, F.G., 2004. Impulsivity: a link between bipolar disorder and substance abuse. Bipolar Disorders 6, 204–212.

Young, R.C., Biggs, J.T., Ziegler, V.E., Meyer, D.A., 1978. A rating scale for mania: reliability, validity and sensitivity. British Journal of Psychiatry 133, 429–435.

PSYCHOGERIATRICS
The Official Journal of the Japanese Psychogeriatric Society

doi:10.1111/psyg.12084 *PSYCHOGERIATRICS* 2014; **14:** 213–221

ORIGINAL ARTICLE

Microstructural abnormality in white matter, regulatory T lymphocytes, and depressive symptoms after stroke

Fumihiko YASUNO,[1,2] Akihiko TAGUCHI,[3,4] Akihide YAMAMOTO,[2] Katsufumi KAJIMOTO,[3] Hiroaki KAZUI,[5] Takashi KUDO,[5] Akie KIKUCHI-TAURA,[6] Atsuo SEKIYAMA,[7] Toshifumi KISHIMOTO,[1] Hidehiro IIDA[3] and Kazuyuki NAGATSUKA[3]

[1]Department of Neuropsychiatry, Nara Medical University, Kashihara, Departments of [2]Investigative Radiology and [3]Neurology, National Cerebral and Cardiovascular Center, [4]Institute of Biomedical Research and Innovation, Foundation for Biomedical Research and Innovation, Kobe, [5]Department of Neuropsychiatry, Osaka University Medical School, Suita, [6]Department of Clinical Research, National Hospital Organization, Osaka Minami Medical Center, Kawachinagano, and [7]Department of Brain Science, Osaka City University Graduate School of Medicine, Osaka, Japan

Correspondence: Dr Fumihiko Yasuno MD PhD, Department of Psychiatry, Nara Medical University, 840 Shijocho, Kashihara, Nara, 634-8522, Japan. Email: ejm86rp@yahoo.co.jp

Received 12 September 2013; revision received 30 April 2014; accepted 4 June 2014.

Key words: *diffusion tensor imaging, fractional anisotropy (FA), magnetic resonance imaging (MRI), post-stroke depression, regulatory T lymphocytes (T_{reg}), stroke.*

Abstract

Background: The purpose of the present study was to investigate the existence of microstructure abnormalities in the white matter circuit in stroke patients and its relationship to depressive episodes. To target the prevention of depression, we also investigated the relationship between lymphocyte subsets and cerebral abnormalities in patients.

Methods: Participants included 18 patients with acute ischemic stroke and 22 healthy control subjects. Diffusion tensor imaging was performed. Whole-brain voxel-based analysis was used to compare fractional anisotropy (FA) between groups. Blood samples were obtained, and the lymphocyte subsets were evaluated using flow cytometry. Follow-up examinations were conducted on 12 patients at 6 months.

Results: FA was decreased in the bilateral anterior limb of the internal capsule in stroke patients. At the 6-month follow-up examination, there was a significant increase in FA, which was associated with a lower depression scale score. Patients showed a decreased percentage of circulated regulatory T lymphocytes, and the degree of reduction was related to the decrease in the FA value in the internal capsule.

Conclusions: FA reductions in the anterior limb of the internal capsule cause abnormality in the frontal-subcortical circuits and confer a biological vulnerability, which in combination with environmental stressors results in the onset of depression. Our findings also demonstrated the possibility of preventing post-stroke depression by targeting the role of regulatory T lymphocytes in brain tissue repair and regeneration after stroke.

INTRODUCTION

Stroke is the third leading cause of death and the most frequent cause of permanent disability in adults worldwide.[1] Depression is common and serious emotional symptom following stroke and is associated with excess disability, cognitive impairment, and mortality.[2] Despite considerable advances in understanding the pathophysiology of cerebral ischemia, therapeutic options for stroke and its related emotional symptoms are still limited. Inflammatory mechanisms activated after brain ischemia represent a key target of current translational cerebrovascular research. Stroke induces profound local inflammatory response involving various types of immune cells that transmigrate across the activated blood–brain barrier to invade the brain.[3]

In attempts to target the prevention of cerebral damage due to stroke, several factors related to inflammation have received considerable attention.[4–6] T lymphocytes are especially central to the development of a sustained inflammatory response in brain injury after a stroke. T cells are sources of pro-inflammatory cytokines and cytotoxic substances, such as reactive oxygen species, in the brain after a stroke; these likely contribute to neuronal death and poor outcomes. However, recent evidence has

indicated a novel role of T cells in promoting brain tissue repair and regeneration in the weeks and months after a stroke.[7] The role of T lymphocytes in ischemic stroke is complex and remains poorly understood. More research is needed to gain a greater understanding of which T-cell subpopulations produce and prevent damage after a stroke.

The primary aim of the present study was to elucidate the microstructural abnormalities in the white matter circuit in stroke patients, as well as their relationship with depressive symptoms after a stroke. When abnormalities were found and a statistical association with post-stroke depressive symptoms was demonstrated, we investigated their relationship with circulating T lymphocytes. For identification of the microstructural abnormalities in stroke patients, diffusion tensor imaging was performed, and whole-brain voxel-based analysis was used to compare fractional anisotropy (FA) between acute ischemic stroke patients and healthy control subjects. Furthermore, we examined which circulating T-cell subpopulations showed differences in stroke patients when compared to healthy subjects and how such T-cell subpopulations are associated with microstructural abnormalities in the white matter of patients.

METHODS

Subjects

After the study was described to subjects, written informed consent was obtained. The study was approved by the medical ethics committee of the National Cerebral and Cardiovascular Center of Japan. The patients, all of whom were of Japanese ethnicity, were recruited from the neurology unit of the National Cerebral and Cardiovascular Center Hospital. These patients had initially been hospitalized for treatment of acute ischemic stroke.

Stroke was diagnosed by neurologists according to the World Health Organization criteria (1989). After the assessment, a group of psychiatrists and neurologists reviewed the data and reached a consensus regarding the presence or absence of psychiatric disease, including dementia according to the Diagnostic and Statistical Manual, 4th edition criteria. Patients were included if they met the following criteria: (i) a focal lesion of either the right or left hemisphere on magnetic resonance imaging (MRI); (ii) absence of other neurologic, neurotoxic, or metabolic conditions; (iii) modest ischemic insult (modified Rankin scale ≤4) with absence of a significant verbal comprehension deficit; and (iv) occurrence of stroke 10–28 days before the examinations. Exclusion criteria included the following: (i) transient ischemic attack, cerebral haemorrhage, subdural haematoma, or subarachnoid haemorrhage; (ii) history of a central nervous system disease such as tumour, trauma, hydrocephalus or Parkinson's disease; and (iii) pre-stroke history of depression. Eighteen subjects met the criteria and participated in this study.

Twenty-two healthy control subjects were recruited locally for this study based on their response to a poster seeking subjects. Exclusion criteria for healthy subjects were a history or present diagnosis of any Diagnostic and Statistical Manual, 4th edition axis I or neurological illness. Major characteristics of this cohort are summarized in Table 1.

All patients were subjected to a neurological examination using the modified Rankin scale (mRS) and the National Institutes of Health Stroke Scale (NIHSS) on the day of the MRI scan.[8,9] A quantitative measurement of cognitive function, the Mini-Mental State Examination (MMSE), and of depressive symptoms, the Hamilton Rating Scale for Depression (HAM-D), was carried out in patients and control subjects. MRI were conducted for all study subjects.[10,11]

At 6 months, follow-up MRI were conducted for 12 of the 18 patients. There were no changes in medication use between baseline and follow-up, and no patients were on antidepressant treatment during the examinations. All patients were subjected to a series of quantitative measurements of depressive symptoms (HAM-D), cognitive function (MMSE), and neurological examination (mRS, NIHSS) on the day of the follow-up MRI scan.[8–11]

Data acquisition of MRI

All MRI examinations were performed with a 3-Tesla whole-body scanner (Signa Excite HD V12M4; GE Healthcare, Milwaukee, WI, USA) with an eight-channel phased-array brain coil. Diffusion tensor images were acquired with a locally modified single-shot echo-planar imaging sequence that used parallel acquisition at a reduction factor of 2 in the axial plane. Imaging parameters were as follows: repetition time = 17 s; echo time = 72 ms; b value = 0, 1000 mm^2/s, acquisition matrix, 128 × 128; field of view, 256 mm; section thickness, 2.0 mm; no intersection gap; 74 sections. The reconstruction matrix was the same as

Table 1 Demographic characteristics of patients and healthy control subjects

Characteristic	Stroke patients (n = 18)	Healthy control subjects (n = 22)	t or χ^2	P-value
Age (years)	70.0 ± 6.7	67.2 ± 5.5	t = 1.46	0.15
Female sex (n)	4 (22.2%)	8 (36.3%)	χ^2 = 0.94	0.33
MMSE score	28.4 ± 1.9	29.3 ± 1.0	t = 1.98	0.06
HAM-D score	2.4 ± 2.4	1.0 ± 1.5	t = 2.20	0.03*
History of disease (n)				
Diabetes mellitus	5 (27.8%)	2 (9.1%)	χ^2_1 = 2.40	0.12
Hyperlipidaemia	5 (27.8%)	1 (4.5%)	χ^2_1 = 4.19	0.04*
Hypertension	14 (77.8%)	5 (22.7%)	χ^2_1 = 12.0	<0.01**
mRS score	1.9 ± 0.7	—		
NIHSS score	2.8 ± 0.9	—		
Anticoagulant or anti-platelet medication (n)				
Warfarin	3 (16.7%)			
Acetylsalicylic acid	13 (72.2%)			
Clopidogrel sulfate	2 (11.1%)			
Cilostazol	3 (16.7%)			
Acute infarcts	1.2 ± 0.5	—		
Volume of acute infarcts (mL)	1.6 ± 0.9	—		
Location of acute infarcts (n)				
Basal ganglia	11 (61.1%)	—	0.611	
Subcortical white matter	6 (33.3%)			
Thalamus	1 (5.6%)	—	0.056	
Laterality of hemisphere infarcts				
Left hemisphere (n)	9 (50.0%)	—		

Data are mean ± SD. *P < 0.05, **P < 0.01.
HAM-D, Hamilton Rating Scale for Depression; MMSE, Mini-Mental State Examination; mRS, modified Rankin scale; NIHSS, National Institutes of Health Stroke Scale.

the acquisition matrix, and 2 × 2 × 2 mm isotropic voxel data were obtained. Motion-probing gradient was applied in 55 directions, the number of images was 4144, and the acquisition time was 15 min 52 s.

To reduce blurring and signal loss arising from field inhomogeneity, we used an automated high-order shimming method based on spiral acquisitions before acquiring diffusion tensor imaging scans.[12] To correct for motion and distortion from eddy current and B_0 inhomogeneity, FMRIB software (FMRIB Center, Department of Clinical Neurology, University of Oxford, Oxford, UK; http://www.fmrib.ox.ac.uk/fsl/fslwiki/) was used. B_0 field mapping data were also acquired with the echo time shift (2.237 ms) method based on two gradient echo sequences.

High-resolution 3-D, T_1-weighted images were acquired with a spoiled gradient-recalled sequence (repetition time = 12.8 ms, echo time = 2.6 ms, flip angle = 8, field of view, 256 mm; 188 sections in the sagittal plane; acquisition matrix, 256 × 256; acquired resolution, 1 × 1 × 1 mm). T_2-weighted images were obtained with a fast-spin echo (repetition time = 4800 ms; echo time = 101 ms; echo train length = 8; field of view = 256 mm; 74 slices in the transverse plane; acquisition matrix, 160 × 160, acquired resolution, 1 × 1 × 2 mm).

Image processing

Fractional anisotropy (FA) maps and three eigenvalues (λ1, λ2, and λ3) were generated from each individual with FMRIB software. First, brain tissue was extracted using the Brain Extraction Tool. Brain maps for each of the 55 directions were eddy corrected, subsequent to which FA values were calculated at each voxel with the FSL FMRIB Diffusion Toolbox.

Image pre-processing and statistical analysis were carried out using SPM8 software (Wellcome Department of Imaging Neuroscience, London, UK). Each subject's echo planar image was spatially normalized to the Montreal Neurological Institute echo planar image template using parameters determined from the normalization of the image with a b value of 0 mm^2/s and the echo planar image template in SPM8. Images were resampled with a final voxel size of 2 × 2 × 2 mm^3. Normalized maps were spatially smoothed using an isotropic Gaussian filter (8-mm full-width at half-maximum).

Voxel-based analysis

Voxel-based analysis was performed using SPM8 software. FA maps were compared between patients and healthy subjects with ANCOVA, with age and sex as covariates of no interest. Statistical inferences were made with a voxel-level threshold of $P < 0.001$, uncorrected, with a minimum cluster size of 100 voxels. The regional FA value was calculated by averaging the FA values for all voxels within the volume of interest corresponding to the cluster composed of significant contiguous voxels. The same volumes of interest were applied to λ_1–λ_3 images, and λ_1–λ_3 values were extracted. Axial (λ_1) and radial diffusivity ($(\lambda_2 + \lambda_3)/2$) were compared.

Flow cytometric analysis of lymphocyte subsets in peripheral blood

Blood samples (5 mL) were obtained from all of the patients and healthy control subjects at the initial examination. The samples were collected into tubes containing sodium heparin. Peripheral blood mononuclear cells (PBMC) were isolated using a Ficoll density gradient (Ficoll-Paque PLUS; GE Healthcare Bio-Sciences AB, Uppsala, Sweden) according to the manufacturer's protocol. PBMC were washed twice with phosphate-buffered saline containing 1% foetal calf serum and 2-mM EDTA.

To identify helper T cells (CD3+ & CD4+), cytotoxic T cells (CD3+ & CD8+), B cells (CD19+) and natural killer cells (CD16+ or CD56+), we incubated the PBMC with fluorescein isothiocyanate-conjugated anti-human CD3 (Beckman Coulter, Orange Country, CA, USA), phycoerythrin-cyanin (PC)5-conjugated anti-human CD4 (Beckman Coulter), PC7-conjugated anti-human CD8 (Beckman Coulter), phycoerythrin-conjugated anti-human CD19 (Beckman Coulter), PC5-conjugated anti-human CD16 (Beckman Coulter), and/or phycoerythrin-conjugated anti-human CD56 (Beckman Coulter) at 4°C for 20 min. To identify regulatory T lymphocytes (T_{reg}) (CD4+, CD25+ & FOXP3+), we incubated the PBMC with fluorescein isothiocyanate-conjugated anti-human CD4 (Beckman Coulter) and PC5-conjugated anti-human CD25 (Beckman Coulter) at 4°C for 20 min. After surface staining, PBMC were fixed, followed by permeabilization and staining with phycoerythrin-conjugated anti-human FOXP3 (Becton Dickinson, Franklin Lakes, NJ, USA) according to the manufacturer's instructions. As negative controls, fluorochrome-conjugated non-specific isotype-matched antibodies (Beckman Coulter) were used. Stained cells were analyzed using a FC500 cytometer and CXP software (Beckman Coulter). Percentages of cells stained with a particular antibody are reported after subtraction of the percentage of cells stained with the relevant negative isotype control antibodies.

Statistical analysis

Group differences in demographic characteristics between patients and healthy controls were examined by unpaired *t*-test and Pearson's χ^2 test. To examine the group differences in FA values and axial/radial diffusivity in volume of interest shown in the voxel-based analysis, we performed ANCOVA with age and sex as covariates.

Paired *t*-tests were performed 6 months after the initial examinations to determine changes in patients' mRS, NIHSS, MMSE, and HAM-D scores and FA values. We performed Pearson's correlation analysis to examine the relationship between FA values and depressive symptoms at the first assessment and at the assessment performed 6 months later. To examine the relationship between the change in depression scale scores and the ratio of the FA values (FA values at second vs initial examination) in patients, we performed Pearson's correlation analysis.

To examine whether the ratio of the FA values was related to the change in depression scale scores (HAM-D scores at second examination minus initial examination), we performed multiple regression analysis after adjustment for age and gender. The change in depression scale scores was the dependent variable, and the ratio of the FA values was the independent variable.

Additionally, we performed ANCOVA with age and sex as covariates to examine the differences in the numbers of helper T cells, cytotoxic T cells, regulatory T cells, B cells, and natural killer cells between patients and healthy control subjects. For the cells showing significant differences between groups, we examined the correlation between FA values and cell number by Spearman's correlation analysis. To determine whether FA values were related to cell number, we performed multiple regression analysis with the FA values as dependent variable and cell number as independent variables, after adjustment for age and gender.

All statistical tests were two-tailed and reported at $P < 0.05$. Bonferroni correction was applied to avoid type I errors due to the multiplicity of statistical analyses. Statistical analysis of the data was performed using SPSS for Windows 19.0 (IBM Japan Inc., Tokyo, Japan).

RESULTS

Demographic and clinical data

Table 1 summarizes the demographic and clinical characteristics of the study subjects. Patients did not differ significantly from healthy control subjects with regard to age, sex, and MMSE scores. As to the history of disease, the ratio of the history of hyperlipidaemia and hypertension was significantly higher in the patients than in the healthy controls. mRS and NIHSS score, anticoagulant or anti-platelet medication, and the location and volume of the infarction among the patients are also shown in Table 1. Patients showed some disability from the stroke at the time of the examination. All of the patients took anticoagulant and/or anti-platelet medicine. Infarctions were located in the basal ganglia (61.1%), subcortical white matter (33.3%), and thalamus (5.6%). There was no significant laterality of hemisphere infarcts.

Comparisons of FA values between groups

In the voxel-based analysis of FA values, the patient and healthy control groups differed in white matter FA values in the left and right anterior limbs of the internal capsule (left anterior limb of internal capsule: (x, y, z) = (–26, 12, 18), cluster voxel size = 831, T value = 5.20; right anterior limb of internal capsule: (x, y, z) = (26, 16, 4), cluster voxel size = 487, T value = 5.24) (Fig. 1a). Figure 1b shows the scatter diagrams of the FA values of the anterior limb of the internal capsule. Table 2 shows the quantification of the differences in FA values and radial/axial diffusivity in these affected regions. These regions revealed decreased axial diffusivity but no change in radial diffusivity.

No patients had lesions in the location of the anterior limbs of the internal capsule. Using Pearson's correlation analysis, we found no significant relationship ($P > 0.05$) between the FA value in the anterior limb of the internal capsule and the volume of infarcts or the severity of stroke shown with mRS and NIHSS scores.

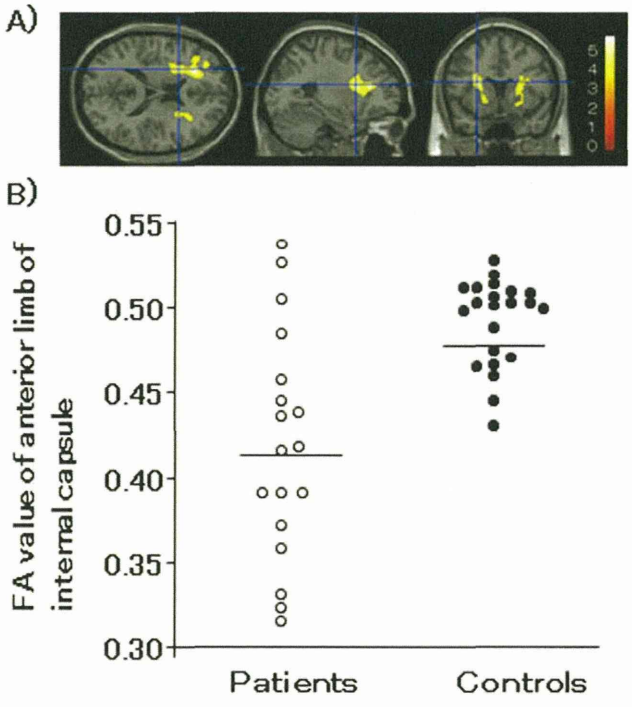

Figure 1 (a) White matter fractional anisotropy (FA) differences in voxel-based analysis comparisons between stroke patients ($n = 18$) and control subjects ($n = 22$). Images are presented in radiological orientation. Statistical parametric mapping projections were superimposed on a representative magnetic resonance image ($x = –26$, $y = 12$, $z = 18$). Patients showed reduced FA in the right and left anterior limbs of the internal capsule. Statistical inferences were made with a voxel-level statistical threshold ($P < 0.001$), uncorrected, with a minimum cluster size of 100 voxels. (b) Scatter plots of FA values in the region of FA reduction of patients and control subjects. Patients' FA values were lower than those of healthy subjects in the bilateral anterior limb of the internal capsule ($P < 0.01$).

Change in FA values of patients after 6 months

Patients showed significantly increased FA values in the anterior limb of the internal capsule 6 months after the infarction (Table 3, Fig. 2a).

There were no significant changes in MMSE and HAM-D scores for either group 6 months after the initial examination (Table 3). There was no significant relationship between FA values and depressive symptoms at the first assessment and at the assessment performed 6 months later. However, we found a significant negative correlation between the increased ratio of the FA values and the change in the scores of depression scales of HAM-D at follow-up 6 months later ($r = –0.67$, $P = 0.02$) (Fig. 2b).

When multiple regression analysis was used to evaluate whether the increased ratio of FA values was